

Redistribution Coefficients of Metal Impurities in Indium Phosphide Grown by Synthesis–Solute Diffusion Technique

Nickolaj V. Lapin & Valerie V. Grinko

Institute of Microelectronics Technology and High Purity Materials, Academy of Sciences, Chernogolovka, Moscow, District 142432, Russia

(Received 16 January 1995; accepted 11 July 1995)

Abstract: Indium inclusion in synthesis–solute diffusion (SSD) grown InP crystals was found to depend on growth temperature and phosphorus vapor pressure and can be described using a calculation model of inclusion on crystallizing with a cellular front. The setup for synthesis employs an electromagnetic mixture of liquid indium, which increases the growth rate up to 1 mm/h, a great improvement on the usual rate of a few millimetres per day. Distribution coefficients of most of harmful impurities that are difficult to remove are measured at an impurity concentration of 10^{-2} mass%. It was shown that purification of the obtained material, removing most impurities, has occurred.

1 INTRODUCTION

Indium phosphide is becoming an increasingly important semiconductor material for microwave and electrooptical application.¹ The development of InGaAsP–InP lattice-matched heterojunctions requires high-quality substrates of both undoped and doped InP.

Because of the high decomposition pressure of InP and high vapor pressure of phosphorus, growth of InP using the liquid-encapsulated Czochralski (LEC) technique is more difficult in comparison with GaAs.² However, use of the synthesis–solute diffusion (SSD) technique^{3–5} has some advantages. The phosphorus vapor pressure and temperature used are lower than in LEC, and the apparatus and process used in LEC are not required. With SSD, it is also easier to control doping of the crystal with volatile impurities. However, data on impurity redistribution on crystallization of InP are quite different.^{6–16}

In the present work, the dependence of In inclusion on the synthesis condition using the SSD method, and the segregation coefficients and solubility limits of some impurities are investigated.

2 EXPERIMENTAL

The synthesis is carried out using a setup previously described.¹⁷ Indium (000s, melt-refined under vacuum) and red phosphorus (5–9s) were introduced into a crucible and on to the edge of silica ampoule, respectively. The charged materials were baked *in vacuo* (2×10^{-6} Torr) at 900°C for indium and 120°C for phosphorus, to remove impurities and water. The silica ampoule was pumped out then sealed and placed into the vertical bizonal furnace with a temperature gradient of 20–30°C/cm. The ampoule was lowered at a rate 1 mm/h. The temperature of indium zone varied from 900 to 1020°C, and low temperature was kept at 400–520°C, yielding a phosphorus vapor pressure of about 3–15 atm³.

A limiting stage was shown² to be the transport of phosphorus through the melting metal in the crucible to the surface, thus obtaining crystals of InP. To intensify this process the setup employs an electromagnetic mixture of liquid indium, which increases the growth rate (v) up to 1 mm/h, compared to the usual rate of a few millimetres per day.^{3,4} The device was constructed on a stator base of electromotor power (0.5 kW), which rotated the

metal mixture at a rate of 300 revs/min. Under setups with varying temperatures, the loading and operational characteristics were measured using a special mechanical mixer. Rotation rate was registered by a photodetector of laser light and a frequency meter.

To determine indium inclusion in InP the samples were cut into equal pieces, which were broken up and dissolved in nitric acid. the included indium was weighed by titrating the obtained solution by Na_2EDTA and recalculating for volume, taking into account the different densities of InP and indium.

Dopants were selected according to their features and electrical activity in InP. They were added to indium first in elemental form (99.99%) to an initial level of 10^{-2} mass%. To define the change in concentration of added impurity along the length of a crystal, samples of InP were cut into sections and the dopant concentration in these crystals was determined by the atomic-absorption method.

3 METAL INCLUSION

Figure 1 shows a plot of indium inclusion quantity (x) as function of synthesis condition. The product of values of phosphorus concentration in liquid indium (C_m) are shown on the x -axis, and slope of the liquidus curve (m)¹⁸ is also given. The quantity of included indium can reach 40% of ingot mass under zone temperatures of 900 and 400°C for indium and phosphorus, respectively. It decreases with increasing metal and phosphorus temperatures

and is not observed at zone temperatures of 1000 and 500°C for indium and phosphorus, respectively.

To estimate the value of x , a suggested¹⁹ model of calculation of inclusion on crystallizing with cellular front is used:

$$\frac{x}{1-x} = \frac{\nu C_m m (1-k)}{DG} - k - (1-k) \exp(-\nu \delta / D) \quad (1)$$

where D is the diffusion coefficient of phosphorus in solution, k is the distribution factor, and δ is the thickness of the boundary diffusion layer.

Calculation using eqn (1) is sensitive to the value of the diffusion coefficient of phosphorus in solution, which at 1000°C varies from 2×10^{-4} to $8 \times 10^{-4} \text{ cm}^2/\text{s}$.²⁰ Therefore, on Fig. 1 data for extreme values of D are plotted (curves 1 and 3). Experimental data (Δ) conform to the area above and correspond with curve 2, calculated for $D = 4 \times 10^{-4} \text{ cm}^2/\text{s}$.

The value of δ is estimated by¹⁹

$$\delta = 3, 24 D^{\frac{1}{3}} \gamma^{\frac{1}{6}} \omega^{-\frac{1}{2}} \quad (2)$$

where γ is the viscosity of liquid indium and ω is the velocity of rotation of the solution. $\omega \simeq 300$ revs/min and $D = 4 \times 10^{-4} \text{ cm}^2/\text{s}$ yield $\delta \simeq 1.2 \times 10^{-2} \text{ cm}^2$. Equation (1) can be modified to give the external value concentration of phosphorus in indium (for $x = 0$):

$$\frac{\nu C_m m}{DG} = \exp(-\nu \delta / D) \quad (3)$$

Points of intersection curves with axes $C_m^* m$ on Fig. 2 correspond to eqn (3).

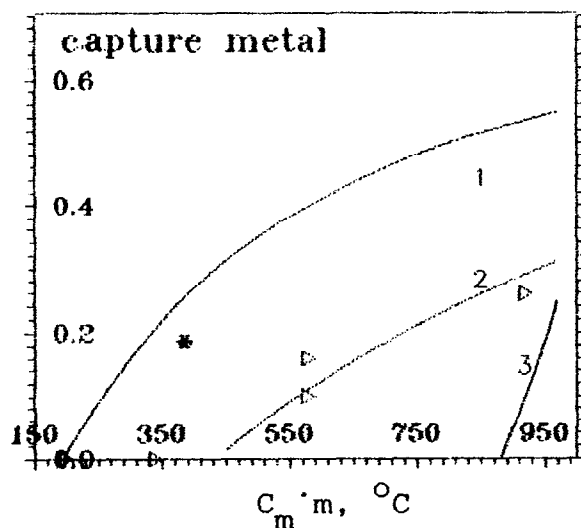


Fig. 1. Dependence of indium inclusion in InP from synthesis condition by SSD: (Δ) and (*), experimental values; (—) calculated values

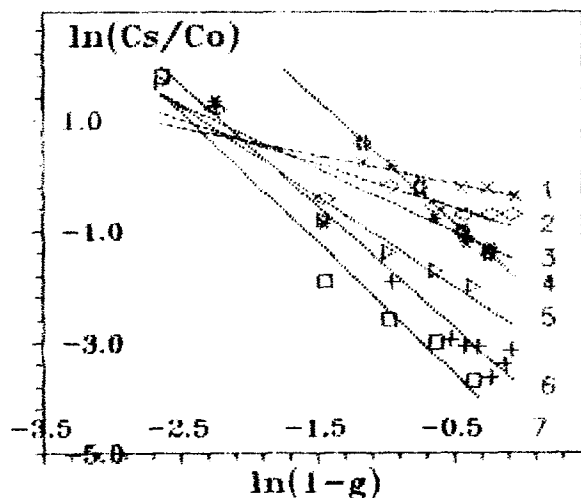


Fig. 2. Distribution of impurities along InP ingot: (1) zinc; (2) sulphur; (3) selenium; (4) cadmium; (5) tin; (6) tellurium; (7) germanium.

It is obvious that under the conditions investigated ($T_{\text{In}} = 1000^\circ\text{C}$, $T_{\text{P}} = 500^\circ\text{C}$) ingots of InP without inclusion are obtained when (v) is 1 mm/h (crystallizing front is smooth). It should be noted that inclusion at synthesis of InP under the same conditions only without an electromagnetic mixture of liquid indium takes place (* in Fig. 1).

4 REDISTRIBUTION OF IMPURITIES

The above-mentioned conditions of the growth of InP without indium inclusion are used to investigate impurity distribution coefficients (k) in a system of solid InP and phosphorus solution in indium.

Experimental data are treated by the well-known normal freeze equation:

$$C_s/C_0 = k(1 - g)^{k-1} \quad (4)$$

where C_0 is the impurity concentration added to the initial indium, C_s is the impurity concentration in solid InP, $g = 1/L$ and is the mass solidified fraction of InP ingot.

Impurities of Group II and VI elements are known to have greater volatility than indium. It is possible to remove the impurities from the reaction zone in the process of crystallization. To avoid this, synthesis is begun upon increasing the phosphorus temperature zone. Phosphorus high pressure of about 10 atm³ prevents impurities from being removed. Also the balance of impurity quantity in InP and initial indium has been taken into account.

Figures 2 and 3 show a linear relationship between experimental $\ln(C_s/C_0)$ and $\ln(1-g)$, indicating the applicability of eqn (4) to this case. It

can be seen that distribution coefficients are less than 1 for each impurity. Coefficient k has been found for each impurity by the tangent of the slope and the ordinate intersection of the curve calculated using the minimization method. If $k \ll 1$, k can be negative then determined by the first case. Because $v = 1$ mm/h at forced mixture melting, obtained value of coefficients are in equilibrium.

This distribution is in contrast to the impurities of Fe, Co, Ni, Cr. Figure 4 clearly shows that the concentration of impurities along the ingot is not changed. This distribution is due to solubility limitation of impurities in InP. The calculated values of solubility limitation are in agreement with known values.^{10,16}

Table 1 summarises known⁶⁻¹⁶ and experimental values of coefficients distribution and solubility limitation.

5 CONCLUSION

Indium inclusion in SSD-grown InP crystals was found to depend on growth temperature and phosphorus vapor pressure and can be described using a calculation model of inclusion on crystallizing with cellular front. Inclusion is not observed at zone temperatures of 1000 and 500°C for indium and phosphorus, respectively.

Distribution coefficients for most of difficult-to-remove harmful impurities are measured on crystallizing indium phosphide at an impurity concentration of 10^{-2} mass%.

It was shown that purification of the obtained material from most impurities takes place, especially in the case of important impurities such as sulphur, selenium and tellurium.

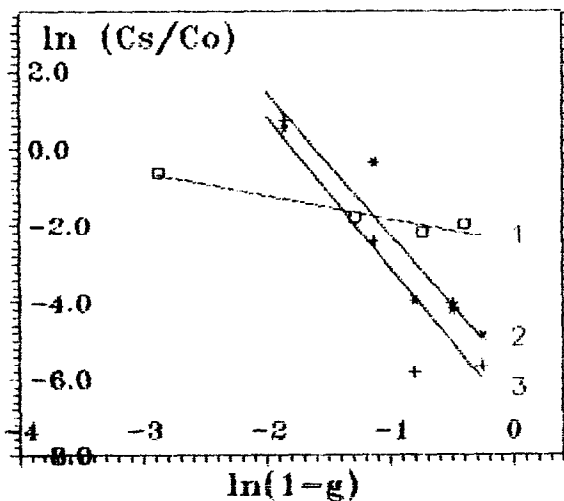


Fig. 3. Distribution of impurities along InP ingot: (1) manganese; (2) silver; (3) copper.

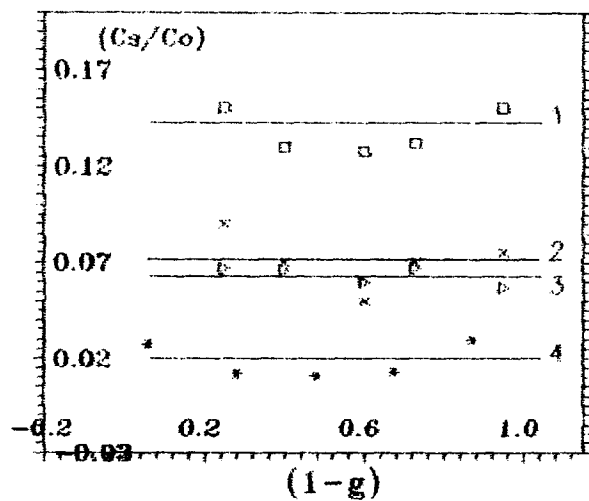


Fig. 4. Distribution of impurities along InP ingot: (1) iron; (2) nickel; (3) cobalt; (4) chrome.

Table 1. Distribution of impurity coefficients on crystallization of indium phosphide

Impurity	Limit solubility of impurities in InP		Distribution coefficients		
	Present paper	Refs 10 and 16	Impurity concentration in Indium, mass% $\times 10^2$	Present paper Distribution coefficient	Czochralski method ⁹⁻¹⁶
Ag	—	—	1.7	0.001	—
Cu	—	—	1.3	0.005	—
Zn	—	—	1.5	0.6	0.7; 0.03; 1.0
Cd	—	—	2.5	0.2	0.1-0.2
Sn	—	—	1.8	0.08	0.02; 0.3; 0.1
Ge	—	—	1.0	0.002	0.4
S	—	—	3.9	0.1	0.46
Se	—	—	3.0	0.1	—
Te	—	—	3.0	0.01	0.38-0.43
Fe	3×10^{-4}	4×10^{-4}	2.3	—	1.6×10^{-3}
Ni	1.5×10^{-3}	—	2.1	—	—
Co	1×10^{-3}	—	1.8	—	4.10^{-5}
Cr	1×10^{-4}	4×10^{-5}	0.78	—	$(1-6) \times 10^{-4}$
Mn	—	1.1×10^{-2}	2.7	0.23	0.4

REFERENCES

1. WISSEMAN, W. R. & FRENSLEY, W. R., *VLSI Electronics Microstructure Science*. Academic Press Inc., UK, 1985.
2. PANISH, M. B., *J. Cryst. Growth*, **27** (1974) 6.
3. BACHMAN, K. J. & BUCHLER, E., *J. Electrochem. Soc.*, **121** (1974) 835.
4. KUBOTA, E. & SUGII, K., *J. Appl. Phys.*, **52** (1981) 2983.
5. KUBOTA, E. & SUGII, K., *J. Cryst. Growth*, **82** (1987) 734.
6. ITO, K. & ITO, H., *J. Cryst. Growth*, **46** (1978) 248.
7. KUPHAL, R., *J. Cryst. Growth*, **54** (1981) 117.
8. ASTLES, M. G., SMITH, F. G. H. & WILLIAMS, E. W., *J. Electrochem. Soc.*, **120** (1973) 1750.
9. NASCHELSKI, A. Ya., JAKOBSON, S. V. & MINAKOV, N. Yu., *Physicochemical Properties of Semiconductor Materials*. Giredmet, Moscow, 1980.
10. LEE, R. N., NORR, M. K., HENTY, R. L. & SWIGGARD, E. M., *Mat. Res. Bull.*, **12** (1977) 651.
11. MIYAZAWA, S. & KOIZUMI, H., *J. Electrochim. Soc.*, **129** (1982) 2335.
12. ANTYPAS, G. A., *J. Cryst. Growth*, **33** (1976) 174.
13. STRAUGHAN, B. W., HURLE, D. T. J., LLOYD, K. & MULLIN, J. B., *J. Cryst. Growth*, **21** (1974) 117.
14. COCKAYNE, B., BROWN, G. T. & MACEWAN, W. R., *J. Cryst. Growth*, **54** (1981) 9.
15. COCKAYNE, B., MACEWAN, W. R. & BROWN, G. T., *J. Cryst. Growth*, **55** (1981) 263.
16. BALLMAN, A. A., NAHORY, R. E. & BROWN, H., *Mater. Lett.*, **1** (1982) 14.
17. LAPIN, N. V., GRINKO, V. V. & NICELSON, L. A., *High Purity Substances*, **0** (1991) 144.
18. TMAR, M., GABRIEL, A., CHATILLON, C. & ANSARA, J., *J. Cryst. Growth*, **68** (1984) 557.
19. LAPIN, N. V. & MALUSOV, V. A., *Doklady Ak. Nauk SSSR Sov. Report Ac. Sci.*, **256** (1981) 650.
20. KOSUSCHKIN, V. G., POTAPOV, V. P. & STRELTSHENKO, S. S., *Electr. Tekh. Sov. Electron. Technique, ser. Mater.*, **9** (1983) 48.